

Crack Growth in the Rail Foot

Senta Pessel¹, Martin Mensinger² and Mathias Gehring³

¹ Technical University of Munich, Munich, Germany, senta.pessel@tum.de

² Technical University of Munich, Munich, Germany, mensinger@tum.de

³ Technical University of Munich, Munich, Germany, Gehring@fs.tum.de

Abstract

Until today the fatigue design of railway rails is based on the assumption that only longitudinal stresses affect the fatigue life of rails. But in recent construction projects it became apparent, that with more slender bridges also the horizontal displacements and subsequently also the lateral forces affecting the rails increase.

The assessment of the load sequence's influence on the crack growth is conducted via fracture mechanical analyses. Using this methodology, crack growth is calculated, starting at an incipient crack. Then different load sequences are applied to the crack, calculating its growth until fracture occurs.

In this paper, first of all the fracture mechanical concepts are introduced. It is shown, how the growth of cracks in the middle and at the edge of the rail foot can be calculated. Then different load spectra are applied to the crack. These load spectra incorporate different train configurations, weather conditions and the two crack locations. Via Markov counting a possibility to easily evaluate long load sequences is introduced.

Keywords: fracture mechanics, rail foot, crack, Markov counting

1. INTRODUCTION

The work for this paper was undertaken in the course of an AiF FOSTA research project granted in 2014. It is a joint research project of the Chair of Metal Structures, the Chair of Concrete Structures and the Chair of Road, Railway and Airfield Construction at the Technical University of Munich.

In the course of the project, the fatigue of continuously welded railway rails subjected to horizontal loads is studied. Currently the fatigue design is carried out using the EN 1991-2. In this design process, only normal and bending stresses are considered. Warping and bending around the weak axle of the section, as they occur in the regions of curves or due to load eccentricities, are not taken into account. In this project fracture mechanical approaches are used in order to find out more about the significance of these additional loads for the crack growth in rail feet.

In this paper first of all a short introduction to the stresses in rails is given. Then the crack growth resulting from different time-series is calculated and the influence of certain impacts is discussed. Finally, a means for the comparison of time series is presented by introducing the method of Markov counting of time series.

2. LOADS ON RAILWAY RAILS

Cracks in railway rails do not solely result from stresses from trains passing the rails. Also other parameters as the temperature, residual stresses and corrosion play a huge role in the lifetime assessment of railway rails. Normally railway rails in Germany are constructed for being fatigue resistant. The loads that have to be taken into account are given in [1]. It states, that besides the stresses from trains, also residual stresses and temperature induced stresses can be found in railway rails. Rails installed in straight tracks or wide curves on macadam superstructure still have a free stress contingent that can be used for taking into account effects from rail-bridge interaction (see also figure 1 (left) for an example).

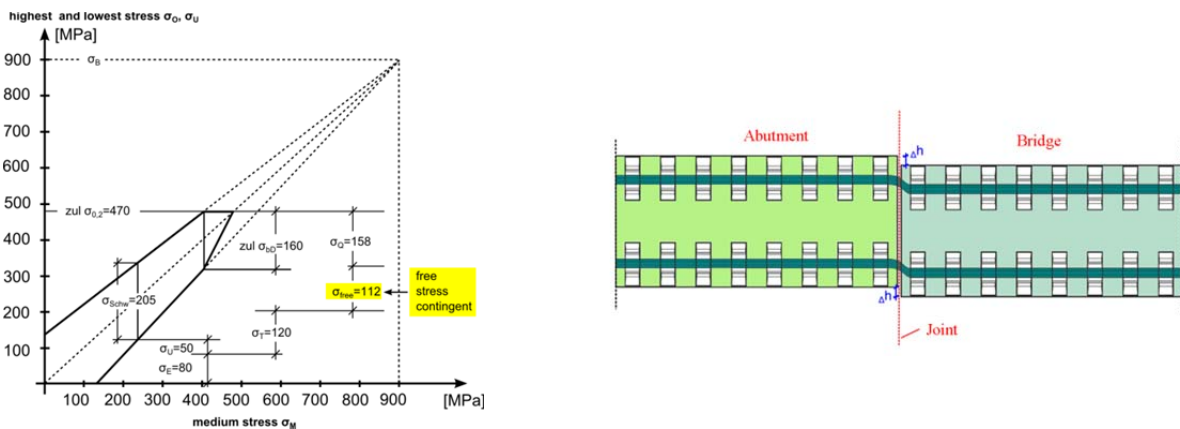


Fig. 1 left: Stress shares in the rail foot (60 E2, 900 N/mm²) from [2]; right: Schematic representation of the lateral displacement Δh by [3]

In [2] a Smith-Diagram collecting all the information is given (see also figure 1 (left)). The disadvantage of this diagram is that only normal and bending stress around the section's strong axle are considered. Lateral movements and torsion of the rail are not taken into account. Schramm showed in [3], how eccentric loads and the lateral movement of bridges lead to increased stresses in the rail foot. The main goal of FOSTA P 1033 is to evaluate the importance of these stresses for the crack growth in the rail foot. Therefore in table 1 different possible load combinations are given [4].

Table 1 Combination of the relevant load components for stresses in the rail foot [4]

| <i>Load component</i> | | <i>location</i> | | |
|--------------------------------------|------------------------------------|-----------------------|--------------|-------------------------------------|
| | | <i>Straight track</i> | <i>Curve</i> | <i>Transition bridge - abutment</i> |
| <i>Train</i> | <i>vertical load</i> | <i>X</i> | <i>X</i> | <i>X</i> |
| | <i>skew track</i> | | <i>X</i> | <i>X</i> |
| | <i>sine run and eccentric load</i> | <i>X</i> | <i>X</i> | <i>X</i> |
| | <i>acceleration / braking</i> | <i>X</i> | <i>X</i> | <i>X</i> |
| <i>Temperature</i> | <i>solar radiation</i> | <i>X</i> | <i>X</i> | <i>X</i> |
| | <i>convection</i> | <i>X</i> | <i>X</i> | <i>X</i> |
| <i>Building</i> | <i>thermal expansion</i> | | | <i>X</i> |
| | <i>lateral displacement</i> | | | <i>X</i> |
| | <i>rotation</i> | | | <i>X</i> |
| <i>Substructure</i> | | <i>X</i> | <i>X</i> | <i>X</i> |
| <i>Rail clamp</i> | | <i>X</i> | <i>X</i> | <i>X</i> |
| <i>Residual stresses of the rail</i> | | <i>X</i> | <i>X</i> | <i>X</i> |

2.1 Stresses Resulting from Trains

In the fatigue design of railway rails on bridges in Germany the EN 1991-2 [1] shall be used for the derivation of the loads. It provides different methods for calculating the stresses in the rails. Probably the most commonly used load model is the so called "load-model 71" consisting of continuous loads and four point loads. Load-model 71 is widely used for static calculations. The stresses obtained can be modified in order to represent regular or heavy traffic as well as dynamic impacts.

As can be seen in 3.1, cracks shall be calculated load-by-load. This is why load-model 71 is not sufficient for fracture mechanical analyses, as it only displays four vertical loads. Therefore the train types displayed in annex D.3 of [1] are used in order to calculate the stresses resulting from trains. In this annex one can choose between regular traffic and heavy traffic. They both incorporate almost the same sum of axle-loads per year, but the regular traffic contains 67 trains where the heavy traffic contains only 51 trains. Thus it's axles are more heavily loaded, which may lead to a faster crack growth in the simulations.

Unfortunately Finite Element calculations of all the axles would be too time consuming. Therefore it was decided to use another possibility to calculate the stresses in the rail foot. The method used is called the Zimmermann-method. It has been developed in Germany and has been extended several times in order to take into account eccentric loads, curves and worn rail heads. The calculations used in this paper can be found in [5].

Originally the method was developed in order to describe the stresses in rails with wooden sleepers. These rails then are approximated as elastically bedded beams. This model only arbitrarily holds with modern constructions for high-speed rails. So the model was fitted to measurement results provided by the Chair of Road, Railway and Airfield Construction at the Technical University of Munich. Figure 2 exemplarily shows stresses induced by the first train of one regular and one heavy traffic, also subjected to residual stresses and stresses from temperature (see table 2 for explication of the nomenclature). In this figure it is easy to distinguish between the different kinds of traffic. Also the differences between the locomotives and the wagons can be seen in the plots.

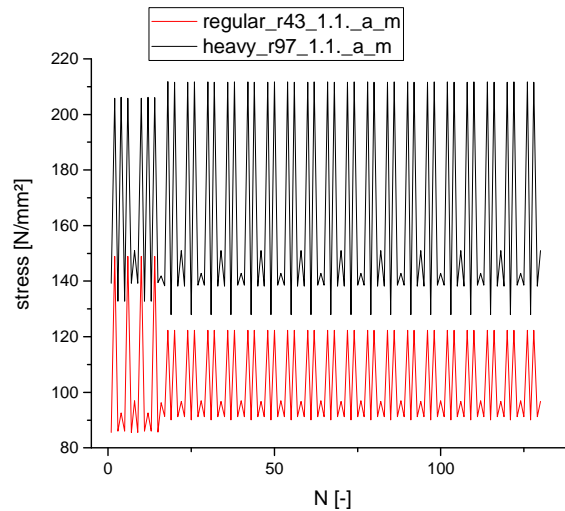


Fig 2 Stresses from the first trains simulated in [5]

2.2 Residual Stresses

In the course of the project, residual stresses in rail samples have been measured. The measurements were conducted by the Chair of Road, Railway and Airfield Construction, using the saw cutting method. Three different rail grades were examined: voestalpine R260 (VA260), voestalpine R350HT (VA350HT) and Moravia Steel R260 (Mo260). All samples belonged to the size category 60E2.

For this paper, two points of measurement are relevant: the middle and the edge of the rail foot. In figure 3 (right) boxplots of the results of the measurements are given. It can easily be seen, that there are tensile stresses in the middle of the rail foot and compressive stresses at the edges of the rail foot. An interesting fact is that the samples of different manufacturers are quite different, whereas there aren't large differences in the respective batches.

For the research project it is assumed, that the residual stresses are not diminished during the rail's lifetime. Therefore they are taken into account in the crack growth calculations. They are added to the stresses from traffic and thus increase/diminish the mean stress. The result of this procedure can be seen in figure 3 (left). In grey the stresses obtained by the calculation of the stresses of one day of regular traffic at a constant temperature of $-30\text{ }^{\circ}\text{C}$ can be seen. In figure 3 (left), the results of the superposition of these stresses with the residual stresses from the middle of the rail foot (minimal and maximal residual stress) are given.

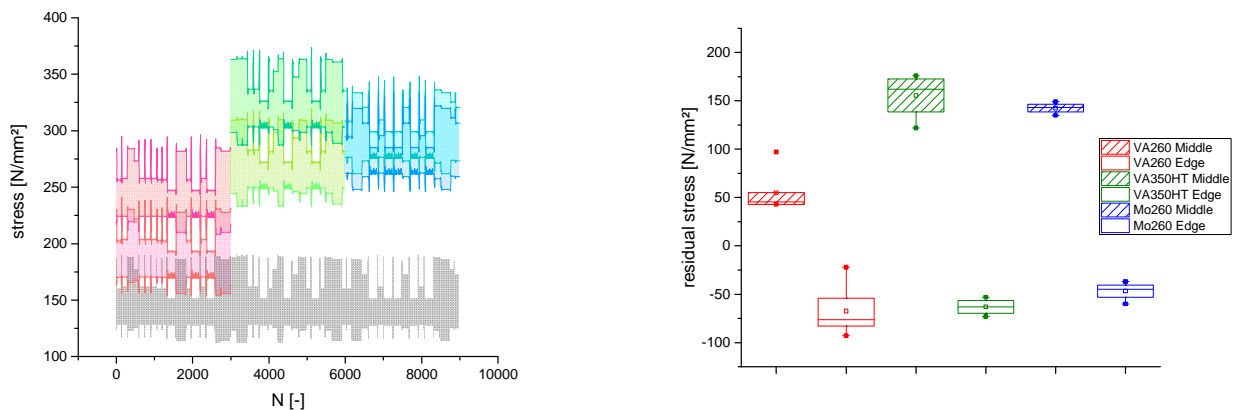


Fig. 3 left: Superposition of stresses from regular traffic and residual stresses at the rail foot (VA260 red, VA350HT green, Mo260 blue); right: box plots of the residual stresses in the rail foot

2.3 Stresses Resulting from Air Temperature and Solar Radiation

In the continuously welded rail strains from temperature change cannot relax, so stresses evolve. In summer, compressive stresses can be found in the rail. As these stresses may lead to buckling of the rail, they are often seen as an inconvenience. But regarding the crack growth in the rails, they also have positive effects, as they diminish the overall stresses and thus decelerate crack growth.

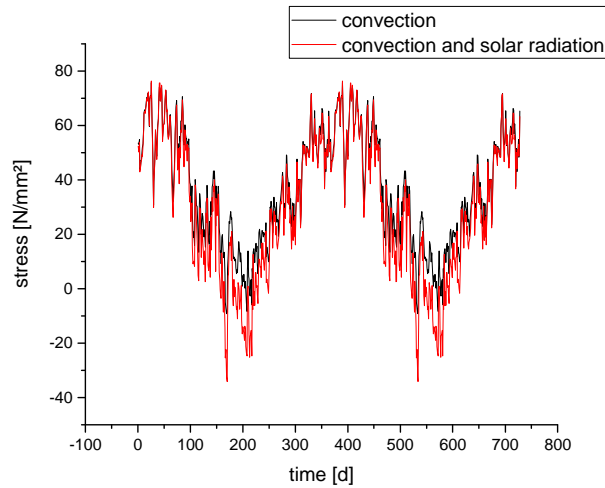


Fig. 4 Stresses in the continuously welded rail , heat transfer convection and radiation + convection

In this paper, two media of heat transfer will be studied: The first is convective heat transfer from the air surrounding the rail and the assumption, that the rail temperature equals the air temperature. The second one is taking into account as well convective heat transfer as solar radiation. The resulting stresses from both alternatives can be found in figure 4. The results of the calculations have been taken from [6].

Day1 in figure 4 is January 1st 2013 at a measuring point in Garching near Munich. Two years with the same temperatures are displayed. It can be observed, that the stresses in the rails considering radiation in winter do not differ from the ones without radiation. The reason for this may be that the sun is quite low in winter, so there are no large energy gains. In summer large differences in the stresses from both calculations can be seen. For the calculations daily average temperatures were used.

3. CONCEPTS OF CRACK GROWTH AND CRACK DESCRIPTION

3.1 Describing Crack Growth

There are three stages of crack growth: Stage 1 is the incipient crack, where crack growth is just beginning. Then there is stage two, the stable crack growth and finally, in stage 3 the instable crack growth. In figure 5 (left) a graphical representation of crack growth taken from [7] can be found. In these graphical representations the scales normally are logarithmic. Then the plot of the crack growth in stage 2 is a straight line. On the abscissa the values for ΔK (the range of the stress intensity factor at the crack tip) can be found. On the ordinate the speed of crack growth (crack growth in [mm per loading cycle]) is given.

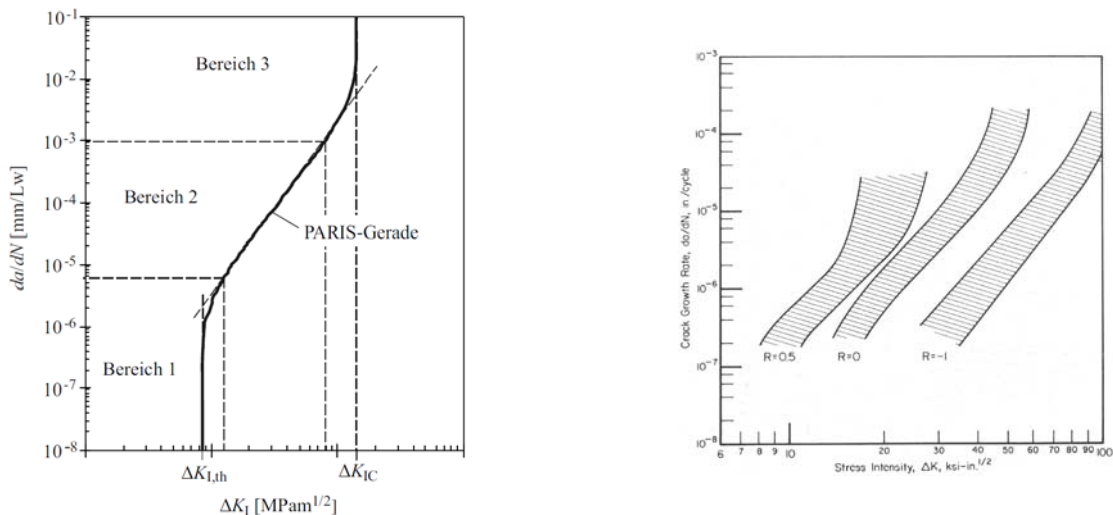


Fig. 5 left: Illustration of the connection of crack speed da/dN and the cyclic stress intensity factor ΔK [7]; Variability of crack growth rate considering R [8]

The most basic formula and also the most widely spread one, is the PARIS-law. It describes the Crack growth in stage 2:

$$\frac{da}{dN} = C (\Delta K)^n \quad (1)$$

Here da/dN describes the speed of crack growth, where da is the progress of the crack after a certain amount of load-cycles dN . The parameters C and n (which is also often called m) represent material values, which have to be determined by experiments. In the experiments it can be shown, that the constants C and n depend on the load ratio applied in the experiments. ΔK is the difference between the maximal and minimal stress intensity factor. This factor can be calculated with the models shown in figure 7. It is a function of the probe's geometry, the loads applied and the depth of the crack. Thus [9] describes da/dN as follows:

$$\frac{da}{dN} = f(\Delta K, R, T, \text{Load, Material, Geometry, ...}) \quad (2)$$

More information about the connections of these parameters can be found in [4].

For load sequences with constant stress amplitudes the service life of a given probe can be calculated via integrating of the PARIS-law. In case of variable amplitudes, step-wise methods have to be employed.

However, the PARIS-law does not cover the full range of crack growth. It only displays stage 2 (the stable portion) of crack growth. Concerning the description of the lifetime of rails, it has another great disadvantage: The Paris law does not take into account the changing of the cracking behavior with changing mean stress or stress ratio. In figure 5 (right) it can be seen, that rail steels display different behavior when they are loaded with R-ratios of 0.5 or 0, where R is defined as $\sigma_{min}/\sigma_{max}$.

In order to describe this R-dependency, the FORMAN-law has been developed. [8] states, that the original FORMAN-law did not describe the test results providing the basis for [8] well. Therefore the following modified FORMAN-law given in [8] is used:

$$\frac{da}{dN} = C (1 - \bar{R})^2 (K_{max}^2 - K_{th}^2) \frac{K_{max}^{n-1}}{K_C - K_{max}} \quad (3)$$

Where

- $\bar{R} = R$ (stress ratio) for $R > 0$, and $\bar{R} = 0$ for $R \leq 0$
- K_{max} Maximum stress intensity factor
- K_{th} Threshold stress intensity factor
- K_C Plane stress fracture toughness

Figure 6 shows the calculation of the crack growth of a crack subjected to two different load sequences. The first sequence spans from 600 to 200 N/mm², the other one spans from 500 to 100 N/mm². So they both display the same $\Delta\sigma = 400\text{N/mm}^2$, but they have a different R-ratio. In figure 6 it can easily be seen, that the two crack growth laws do not yield the same results. The Modified FORMAN equation yields larger crack growth rates than the PARIS-law. The latter one does not show any dependency of the maximal stresses or the R-ratio, as it is only dependent on $\Delta\sigma$. Thus it would not be sufficient for the further work, only to work with the PARIS-law.

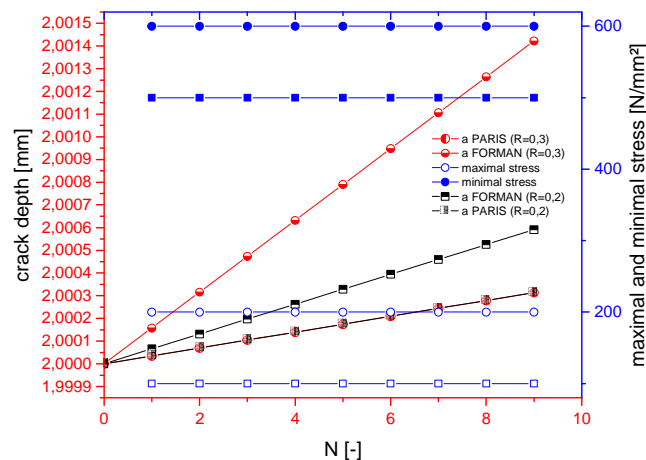


Fig. 6 crack growth with the PARIS-law and the modified FORMAN-law

3.2 The Choice of Crack Model

In the research project, cracks in the rail foot shall be described. There are two locations, where cracks are likely to grow in the rail foot: The middle of the rail foot and the edges of the rail foot. A rough approximation of the rail foot's geometry is a flat, very long plate. For such plates Newman and Raju developed solutions for calculating the stress intensity factors K in [10] and [11]. In figure 7 the crack models and photos from cracks found after Wöhler testing real rails are shown.

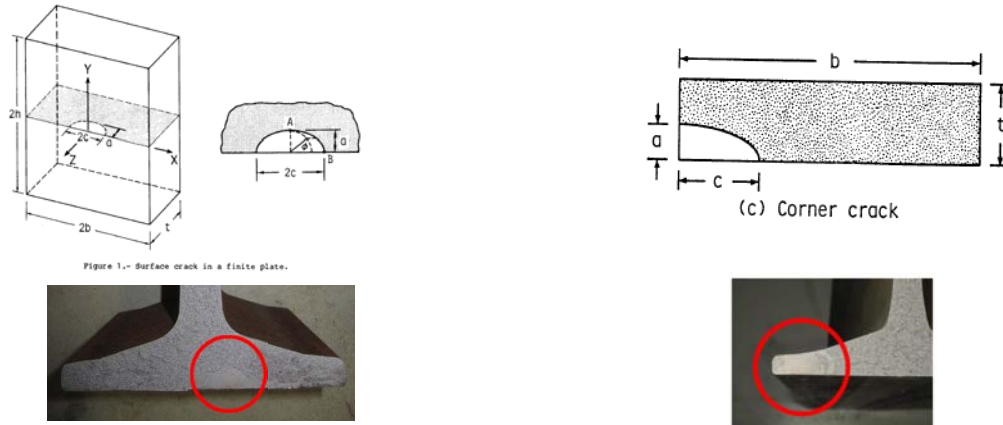


Figure 1.- Surface crack in a finite plate.

Fig. 7 Crack model for a plate with a semi-elliptical surface crack in the middle of the plate (left) [10] and a quarter-elliptical surface crack at the edge of the plate (right) [11]. Underneath photos of real test specimen showing such cracks are displayed.

4. IMPACT OF DIFFERENT LOAD SEQUENCES ON THE CRACK GROWTH

In order to evaluate the difference that the change of the load sequence makes on the crack growth, different crack growth simulations have been made. The nomenclature and parameters used are shown in table 2. It must be stressed, that the simulations undertaken do not yet represent crack growth in rails, but crack growth in slim plates subjected to railway-loads. Finite element simulations of cracks in railway rails suggest that they behave differently from the plates and that the models shown in figure 7 have to be adapted for the present problem. Another important point is, that the initial crack depth has been chosen very deep so that the simulations show results without consuming too much simulation time. Crack depths like these won't often occur in the real life of a railway rail.

Table 2 parameters of the simulations

| Crack location | Traffic | Residual stress N/mm ² | Date | Medium of heat transport | Name |
|----------------|---------|--------------------------------------|------|--------------------------|-----------------------|
| middle | heavy | 97 | 1.1. | air | heavy_r97_1.1._a_m |
| | | 97 | 1.1. | air + radiation | heavy_r97_1.4._a_m |
| | | 97 | 1.4. | air | heavy_r97_1.1._a+c_m |
| | regular | 43 | 1.1. | air | regular_r43_1.1._a_m |
| | | 97 | 1.1. | air | regular_r97_1.1._a_m |
| edge | regular | 176 | 1.1. | air | regular_r176_1.1._a_m |
| edge | regular | 97 | 1.1. | air | regular_r97_1.1._a_e |

In all simulations the attempt so simulate one year of crack growth was made. The results of the crack growth simulations can be seen in figure 8. Regarding the results it can be seen, that there are huge differences in the lifetimes reached in the simulations. One year of simulation time could not always be reached. Also the crack depths reached differ.

The first main influence on the crack growth pointed out here is the influence of residual stresses. There are three simulations of regular traffic that only differ in the residual stresses taken into account. It can be seen, that the simulation with 43 N/mm² residual stress almost doesn't yield any crack growth at all. On the contrary the simulation with 176 N/mm² already stops after a short time of crack growth, because the K_{max} exceeds K_{Ic} . It becomes apparent, that the mean stresses play a huge role when crack growth is investigated.

The heavy traffic also breaks the plate before the year passed. Although the weight transported in one year is almost the same in regular and heavy traffic, the heavy traffic yields higher crack growth rates. Also seasonal differences can be made out: The green and the red heavy traffic started both on January 1st, whereas the point of origin for the black heavy traffic chosen as April 1st. It can be seen, that the black crack growth starts more slowly because of the smaller stresses in summer.

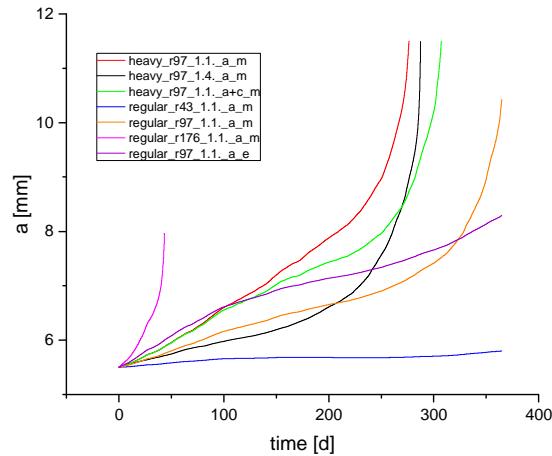


Fig. 8 Crack growth in a plate in one year

The magenta curve shows the crack growth of an edge specimen. It can be seen, that it's crack growth is faster than the crack growth of the matching middle crack. But in this case one has also to refer to figure 3, where the location's residual stresses are shown. Looking at this figure it becomes apparent, that 97 N/mm² residual stress won't be found in the regions of the rail foot's edges, so crack growth there will be slower in reality than in this simulation.

5. CHARACTERIZATION OF LOAD SERIES

One can see from section 4, that the load series are even more important for the crack growth than the location of the crack. This is why possibilities to visualize the time series were probed. Looking at figure 4 it becomes apparent, that the visualization of the time series itself yields no good indicators, as it becomes difficult to distinguish the differences between the time series.

The means used here was Markov counting of the time-series. In order to use this method, first of all the time series has to be divided into classes. Then every turning point of the time series is assigned to one class. After that the graded time series is searched point by point and the way from one turning point to the next is saved in the Markov matrix. The main diagonal stays empty. Above it (in the upper right corner) the load steps from a minimum to a maximum can be found. The lower left side is almost symmetrical to the upper side and displays steps from a maximum to a minimum.

In figure 9 the Markov matrices of two regular traffics are shown. It can be seen, that the matrices do not change very much due to the different superposed residual stresses. The main change is the shift of the matrix along the main diagonal. With this (and taking into account figure 8) it may be concluded, that time series with the potential to induce faster crack growth are rather shifted to the lower right corner of the Markov matrix.

Figure 10 shows the Markov-matrices of two heavy traffics. A clear difference to the regular traffics in figure 9 can be seen. The entries of the matrices are shifted away from the main diagonal, which indicates higher stresses.

The time series of heavy traffic were simulated with different stresses from temperature. The left simulation only incorporated convective heat transfer, whereas the figure on the right displays the superposition with temperatures from convection and radiation. It can be observed, that the superposition with the stresses from convection and radiation elongates the matrix along the main diagonal. This makes sense, as temperature changes are also a change of mean stresses.

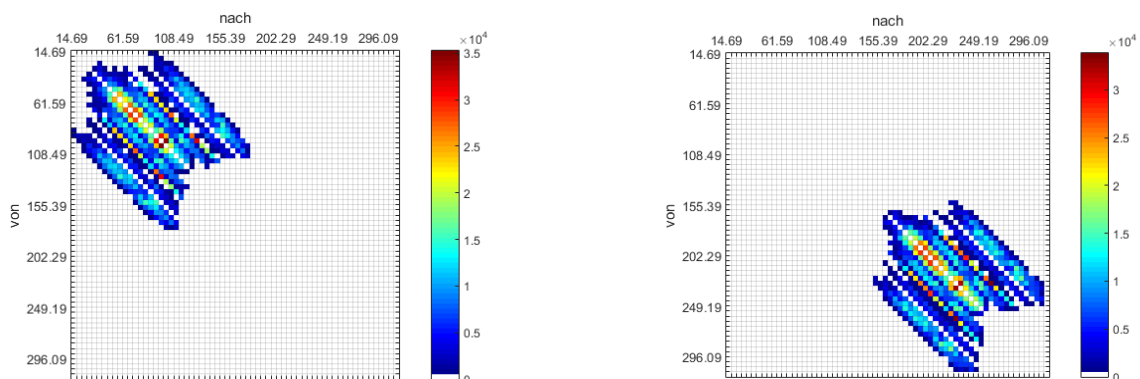


Fig. 9 left: Markov-matrix of regular_r43_1.1_a_m, right: Markov-Matrix of regular_r176_1.1_a_m

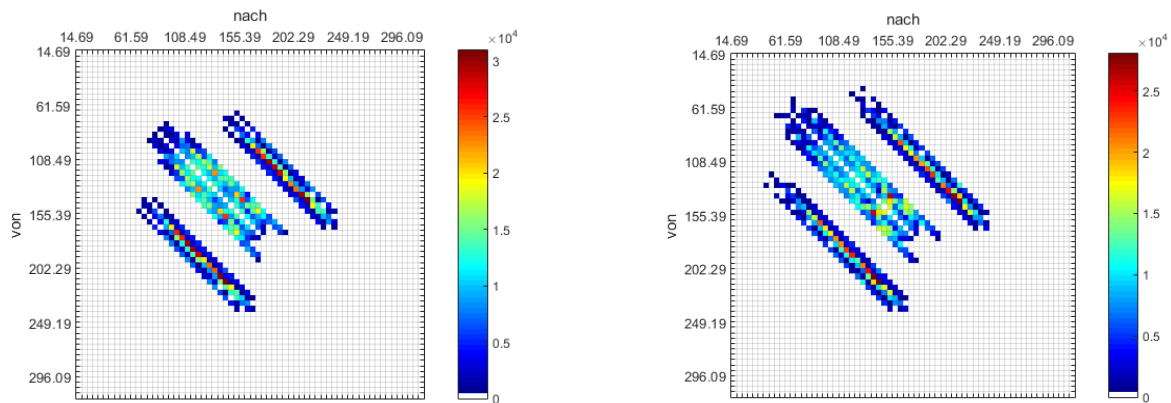


Fig. 10 left: Markov-matrix of heavy_r97_1.1_a_m, right: Markov-matrix of heavy_r97_1.1_a+c_m

6. CONCLUSIONS AND OUTLOOK

In this paper it was shown that different load spectra have a different influence on crack growth. Especially shifts in the mean stresses have huge impacts on the residual life of a crack. Therefore crack simulations for railway rails should be made with the FORMAN-law, taking into account the stress ratio R . More accurate results can be obtained, if additional stresses such as stresses from temperature changes or lateral displacements are considered for short time sequences. Markov matrices were established as means for the evaluation of time series.

In further works closer investigations on the matching of Markov matrices with the results of crack growth simulations will be undertaken. Also refined simulations of the crack growth at the edges of the rail foot will be made.

7. ACKNOWLEDGEMENTS

The work presented is carried out as part of a joint research project (2014-2016). This project P1033 of the research association (FOSTA) was financed over the AiF within the development program for industrial community research and development (IGF-Nr. 18094N) from the Federal Ministry of Economic Affairs and Energy (BMWi) based on a decision of the German Bundestag. The authors thank all partners for their cooperation. Also to the supporting companies special thanks are given.

The data for the stresses from differing temperature have been provided by the Meteorological Institute Munich, which is an Institute of the Ludwig-Maximilians-Universität in Munich.

8. REFERENCES

- [1] DIN EN 1991-2:2010. „Eurocode 1: Einwirkungen auf Tragwerke – Teil 2: Verkehrslasten auf Brücken“; Deutsche Fassung EN 1991-2:2003+AC:2010. DIN – Deutsches Institut für Normung. Dezember 2010
- [2] Freystein, H., 2012. „Untersuchungen zu den zulässigen zusätzlichen Schienenspannungen aus Interaktion Gleis/Brücke“. Dissertation. Technische Universität Berlin. 2012
- [3] Schramm, N., 2014. „Beitrag zur wirklichkeitsnahen Ermittlung von Schienenspannungen im Übergangsbereich zu Brückentragwerken“. Technische Universität München, Lehrstuhl für Massivbau. Master’s Thesis. 2014.
- [4] Pessel, S., Mensinger, M., 2016, “Fracture mechanics based approach to the significance of certain loads on the service life of rails”, *Transportation Research Procedia* 14, 2016, pp. 2006-2014, doi: 10.1016/j.trpro.2016.05.168
- [5] Hu, Wen, 2016, “Einfluss von Lastausmitteln und Rissinitiierungsort auf die Restlebensdauer von Eisenbahnschienen”, Master’s Thesis, Chair of Metal Structures, Technical University of Munich
- [6] He, Jiajing, 2015, “Rissfortschritt in Schienenfußmitte unter Berücksichtigung von Temperatur- und Eigenspannungsschwankungen”, Master’s Thesis, Chair of Metal Structures, Technical University of Munich
- [7] Richard, H., Sander, M., 2009. “Ermüdungsrisse”. Vieweg+Teubner I GWV Fachverlage GmbH, Wiesbaden
- [8] Rice, R. C., Leis, B. N., and Tuttle, M. E., “An Examination of the Influence of Residual Stresses on the Fatigue and Fracture of Railroad Rail”, *Residual Stress Effects in Fatigue*, ASTM STP 776, American Society of Testing and Materials, 1982, pp. 132-157
- [9] Deutscher Stahlbau-Verband, 1996. “Stahlbau Handbuch”. Stahlbau-Verlagsgesellschaft mbH. Köln. 1996.
- [10] Newman, J. C., Jr., Raju, I. S., 1979, “Analyses of Surface Cracks in Finite Plates Under Tension or Bending Loads”, NASA Technical Paper 1578
- [11] Newman, J. C., Jr., Raju, I. S., 1984, “Stress-Intensity Factor Equations for Cracks in Three-Dimensional Finite Bodies Subjected to Tension and Bending Loads”, NASA Technical Memorandum 85793